attributed to the change in the magnetostatic energy of the domain caused by the relation of the temperature-dependent M_C to the stability of the formation of the bubble domain (*1*). The elongated domain is transformed into the collapse of the bubble domain as M_C is decreased (Fig. 1, D and F), because H_W increases and H_D decreases with decreased M_C, leading to the instability of the domain as a result of decreasing magnetostatic energy. For the formation of the bubble domain at 72 K, the important factor is not only the value of M_C but also the thin domain originating in the large anisotropic crystalline structure. If the domain is thicker, the elongated domain will appear because H_D increases with increasing t. The balance between the appropriate value of M_C and the thickness of the domain is preserved for the stable formation of the bubble domain at 72 K.

At 87 K, a steep structure appears with a larger absolute value of B_z than that at lower temperatures (Fig. 1G). In this temperature range, the magnetic moments nearly lie in the MnO_2 plane. Therefore, the structure represents a stray field arising from the boundaries of magnetic domains with in-plane magnetization. At 97 K, the B_z value of the observed structure is increased because of further tilting of the magnetic moments toward the MnO_2 plane (Fig. 1H). The size of the domain is nonuniform.

The observed close-packed bubble domain in the structure is promising for high-density magnetic recording. Removing the need for an external magnetic field for the generation of the domain provides a cost incentive for the downsizing of the device. In terms of its practical application, the bubble domain structure obtained in this study is still limited in temperature range; moreover, the size of the domain is not small enough. Further optimization of the material should be achieved through raising the temperature of the stable formation of the smaller bubble domains, either by finding a new composition for the layered structure or by fabricating an artificial layer structure.

References and Notes

1. A. H. Bobeck and E. Della Torre, *Magnetic Bubbles* (North-Holland, Amsterdam, 1975).
2. C. Kittel, *Rev. Mod. Phys.* **21**, 541 (1949); B. Kaplan and G. A. Gehring, *J. Mag. Mag. Mat.* **128**, 111 (1993).
3. Y. Moritomo, A. Asamitsu, H. Kuwahara, Y. Tokura, *Nature* **380**, 141 (1996).
4. T. Kimura *et al.*, *Science* **274**, 1698 (1996).
5. T. Kimura, A. Asamitsu, Y. Tomioka, Y. Tokura, *Phys. Rev. Lett.* **79**, 3720 (1997).
6. R. H. Heffner *et al.*, *ibid.* **81**, 1706 (1998).
7. T. G. Perring, G. Aeppli, T. Kimura, Y. Tokura, M. A. Adams, *Phys. Rev. B* **58**, R14693 (1998).
8. T. Fukumura, thesis, University of Tokyo (1998).
9. Q. Lu, C.-C. Chen, A. de Lozanne, *Science* **276**, 2006 (1997).
10. H_W and H_D are defined as follows:

$$H_W = \sigma_W/(dM_S)$$

where σ_W is domain wall energy per unit area.

$$H_D = 8M_S(1 + d^2/t^2)^{1/2} E(k, \pi/2) - 8dM_S/t$$

where

$$E(k, \pi/2) = \int_0^{\pi/2} (1 - k^2 \cos^2 \theta)^{1/2} \, d\theta$$

and $k = (1 + t^2/d^2)^{-1/2}$. H_B is given by the magnetic field from the rectangular parallelepiped magnet with magnetization of M_S and dimension of $d \times d \times t$.

11. Supported by Core Research for Evolutional Science and Technology (CREST) of the Japan Science and Technology Corporation (JST) and by The New Energy and Industrial Technology Development Organization (NEDO), Japan.

11 March 1999; accepted 11 May 1999

Century-Scale Shifts in Early Holocene Atmospheric CO_2 Concentration

Friederike Wagner,[1] Sjoerd J. P. Bohncke,[2] David L. Dilcher,[3] Wolfram M. Kürschner,[1] Bas van Geel,[4] Henk Visscher[1]

The inverse relation between atmospheric carbon dioxide concentration and stomatal frequency in tree leaves provides an accurate method for detecting and quantifying century-scale carbon dioxide fluctuations. Stomatal frequency signatures of fossil birch leaves reflect an abrupt carbon dioxide increase at the beginning of the Holocene. A succeeding carbon dioxide decline matches the Preboreal Oscillation, a 150-year cooling pulse that occurred about 300 years after the onset of the Holocene. In contrast to conventional ice core estimates of 270 to 280 parts per million by volume (ppmv), the stomatal frequency signal suggests that early Holocene carbon dioxide concentrations were well above 300 ppmv.

The records of the relation of greenhouse gases to Quaternary climate change come largely from ice cores from Antarctica and Greenland. Trends in the atmospheric CO_2 amount parallel those of the temperature inferred from the isotopic compositions of oxygen ($\delta^{18}O$) and hydrogen (δD) during the past 250,000 years, showing that variation in greenhouse gas concentrations is an important factor in long-term glacial-interglacial climate evolution (*1*). Carbon dioxide data from ice cores also seem to correlate with millennial-scale temperature changes (*2*). However, a correlation of atmospheric CO_2 amounts to century-scale climate shifts in the Holocene (*3, 4*) is still unclear. Most of the Holocene ice core records from Antarctica do not have adequate temporal resolution (*5*). In Greenland ice, the Holocene CO_2 concentrations are generally considered to be influenced by postdepositional enrichment (*6*). Because of the apparent inadequacies and controversies in the CO_2 records derived from ice sheets, alternative methods have to be developed to improve the accuracy of detecting and quantifying possible short-term shifts in the Holocene atmospheric CO_2 regime. Here, we provide a century-scale record of early Holocene atmospheric CO_2 amounts, based on a stomatal frequency analysis of leaves that were buried in peat deposits.

An analysis of herbarium material collected over the past 200 years and controlled growth experiments under preindustrial CO_2 amounts (*7, 8*) has shown that, for Northern Hemisphere tree species, stomatal frequency decreases linearly as atmospheric CO_2 concentration increases. A near-annual analysis of a 40-year record of the buried leaves of a solitary growing birch (*Betula pendula*) has illustrated that deciduous trees are equipped with a plastic phenotype, capable of a lifetime adjustment of stomatal frequency to an increase in anthropogenic CO_2 (*9*).

Stomatal frequency is conventionally expressed in terms of stomatal density and stomatal index (SI) (*10*). In contrast to stomatal density, SI expresses frequency changes independently of variation in epidermal cell size and therefore is the more sensitive parameter for detecting stomatal frequency response to changes in CO_2 concentration (*11*). The effects of intrinsic variation in SI values within and among leaves of an individual tree species (*11, 12*) can be accounted for analytically, allowing the replication of temporal trends of mean SI values (*9, 13*). At least for European tree birches (*B. pendula* and *B. pubescens*), field studies and controlled-envi-

[1]Laboratory of Palaeobotany and Palynology, Utrecht University, Budapestlaan 4, 3584 CD Utrecht, Netherlands. [2]Netherlands Centre for Geo-ecological Research, Faculty of Earth Sciences, Free University, De Boelelaan 1085, 1081 HV Amsterdam, Netherlands. [3]Paleobotany Laboratory, Florida Museum of Natural History, University of Florida, Gainesville, FL 32611, USA. [4]Netherlands Centre for Geo-ecological Research, Department of Palynology and Paleo/Actuo-ecology, University of Amsterdam, Kruislaan 318, 1098 SM Amsterdam, Netherlands.

ronment experiments show that CO_2-induced trends in mean SI values are not substantially disturbed by influences of environmental factors such as light, temperature, and nutrient supply (*14*). Calibrated against the Mauna Loa record of CO_2 increase (*15*), mean SI values for individual tree species may be empirically modeled as a function of changing atmospheric CO_2 concentrations (*16*). Response curves can be efficiently applied in the quantification of time-series data on stomatal frequency derived from fossil leaves of extant tree species. Long-term stomatal frequency changes in fossil leaves correlate with general glacial-interglacial CO_2 dynamics (*17*) and have been used to estimate atmospheric CO_2 concentrations in the late Miocene, Pliocene, and early Pleistocene (*8*).

We studied leaf material from a peat section that was temporarily exposed at the Borchert archaeological site near Denekamp, northeastern Netherlands (*18*). The sequence covers part of the Late Glacial (Younger Dryas) and the Holocene. We collected leaves of European tree birches (*B. pendula* and *B. pubescens*) from 16 horizons of the early Holocene (Preboreal) part of the section. Regionally, the Preboreal is subdivided into the Friesland phase, the Rammelbeek phase, and the Late Preboreal (Fig. 1A). Characterized by the spread of tree birches, the Friesland phase marks the rapid expansion of woodland at the beginning of the Holocene. Six ^{14}C dates suggest an average sampling resolution of 40 to 50 years.

Leaves of *B. pendula* and *B. pubescens* display essentially similar SI patterns (*16*). In stomatal frequency analysis, therefore, the mixed fossil assemblage of leaves of tree birches from the Borchert section can be treated as a single category (Fig. 1A). We used the rate of historical CO_2 responsiveness of tree birches (Fig. 2) to derive a Preboreal atmospheric CO_2 record based on the mean SI values for the fossil leaf remains. In the Friesland phase, inferred CO_2 concentrations of 265 ± 21 and 260 ± 25 parts per million by volume (ppmv) are followed by a rapid rise to 327 ± 10 ppmv and a more gradual increase to a maximum of 336 ± 8 ppmv in the early part of the Late Preboreal. Then, there is a continuous CO_2 decline to a minimum of 301 ± 21 ppmv, followed by a sharp increase to 348 ± 14 ppmv. In the uppermost part of the studied interval, CO_2 concentrations stabilize again to values between 333 ± 8 and 347 ± 11 ppmv.

The initial decrease of the SI in the Friesland phase suggests that atmospheric CO_2 concentrations rose by ~65 ppmv in less than a century. The CO_2 increase occurred during prominent environmental changes, which are reflected in the lithology and the palynological record (*18*). Basal gyttja formation is followed by a rapid hydroseral succession at the formerly open water site at this time. Regional woodland expansion is reflected by an increase in *Betula* pollen and the occurrence of *Betula* macrofossils. Both the CO_2 increase and the environmental changes at this site correlate with the global climate amelioration at the beginning of the Holocene.

Because of the lack of leaf material from the lowermost part of the section, the onset of the CO_2 rise could not be exactly determined. Yet, the general timing of the rise is in agreement with the CO_2 record from the Antarctic Byrd ice core (*19*), where the Younger Dryas–Holocene transition is defined by a sudden CO_2 increase from 260 to 280 ppmv. In our SI-based reconstruction, the magnitude of the rise is higher, resulting in CO_2 concentrations well above 300 ppmv. There is a clear covariation (Fig. 1B) between the reconstructed CO_2 increase and the rapid positive $\delta^{18}O$ shift that

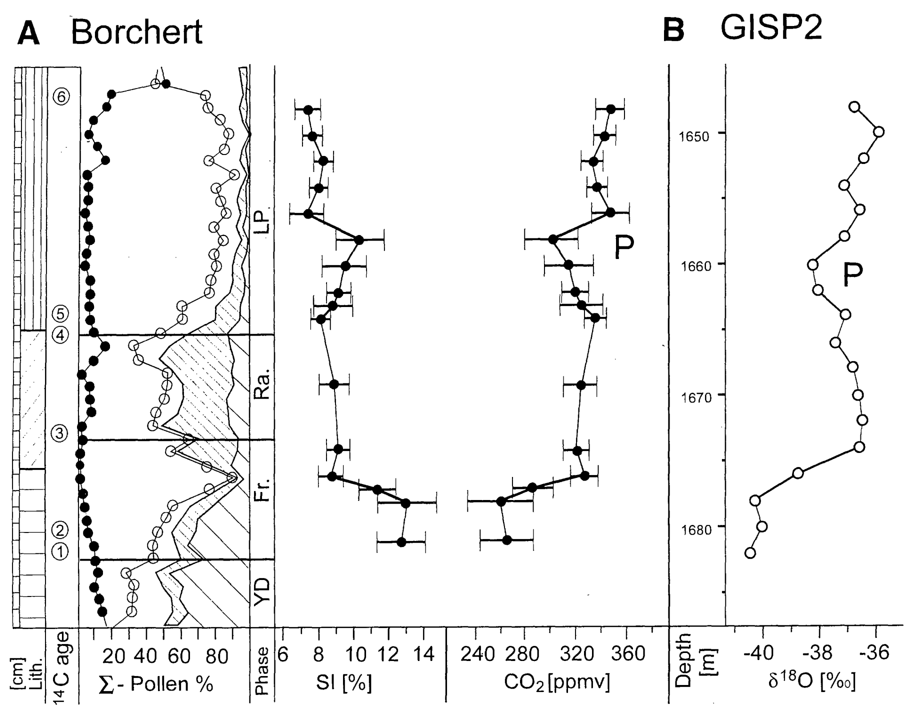

Fig. 1. (**A**) Mean SI values (±1σ) for *B. pendula* and *B. pubescens* from the early Holocene part of the Borchert section (Netherlands; 52.23°N, 7.00°E) and reconstructed CO_2 concentrations. The scale of the section is in centimeters. Three lithological (Lith.) units can be recognized (*18*): a basal gyttja (=), succeeded by *Drepanocladus* peat (//), which is subsequently overlain by *Sphagnum* peat (|||). Six conventional ^{14}C dates (in years before the present) are available (indicated by circled numbers): 1, 10,070 ± 90; 2, 9930 ± 45; 3, 9685 ± 90; 4, 9770 ± 90; 5, 9730 ± 50; and 6, 9380 ± 80. Summary pollen diagram includes arboreal pollen (white area) with *Pinus* (●) and with *Betula* (○) and nonarboreal pollen with Gramineae (\\\\\\) and with Cyperaceae, upland herbs, and Ericales (\\ \\). Regional climatic phases after (*18*): YD, Younger Dryas; Fr., Friesland phase; Ra., Rammelbeek phase; and LP, Late Preboreal. For analytical method, see (*13*). Quantification of CO_2 concentrations according to the rate of historical CO_2 responsiveness of European tree birches (Fig. 2). P indicates the reconstructed position of the Preboreal Oscillation. (**B**) $\delta^{18}O$ profile for the Younger Dryas–Holocene transition in the Greenland GISP2 ice core, after (*20*); P denotes the $\delta^{18}O$-inferred cooling of the Preboreal Oscillation, starting at ~11,300 calendar years before the present (*3*).

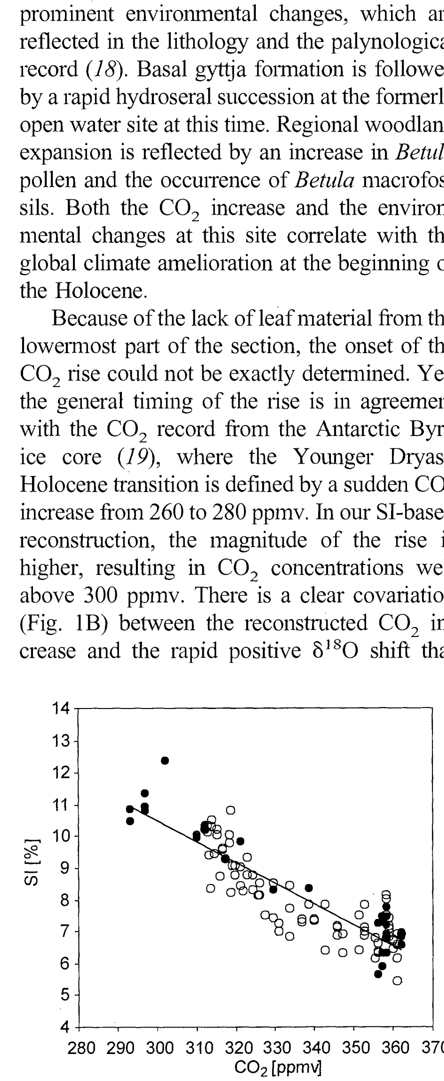

Fig. 2. Relation of mean SI for *B. pendula* (○) and *B. pubescens* (●) to the global atmospheric CO_2 increase in the period from 1896 to 1998. The historical training set for the European tree birches consists of 105 samples, originating from presently accumulating peat (*9*) supplemented by herbarium and field material. For analytical method, see (*13*). Mean historical CO_2 concentrations are derived from Mauna Loa monitoring (*15*) and Antarctic shallow ice core data (*24*). Mean SI values show a linear decrease from 11% at 290 ppmv to 6.4% at 360 ppmv CO_2 [n = 105; slope = −0.065; goodness-of-fit linear model: R^2 = 0.78, R^2_{adj} = 0.78; analysis of variance results $F(1, 103)$ = 384.97 (P < 0.000); statistics performed with SPSS 7.5 for Windows (Statistical Product and Service Solutions, Chicago, Illinois)].

characterizes the onset of Holocene warming in high-resolution isotope records from Greenland ice (*20*).

About three centuries after the initiation of Holocene warming, a $\delta^{18}O$ minimum in Greenland ice reflects a short cooling event (Fig. 1B). A 150-year climate deterioration has also been deduced from numerous terrestrial and marine biorecords (*21*). Although exact dating of the non–ice core records is hampered by the occurrence of ^{14}C-age plateaus during the early Holocene, multiproxy analysis suggests that all reported events collectively reflect the Preboreal Oscillation (*3*). In the Borchert section, the reconstructed CO_2 values drop from ~340 to ~300 ppmv at this time (Fig. 1A). A relation between CO_2 dynamics and the Preboreal Oscillation had been suspected on the basis of an abrupt rise in the early Holocene $\Delta^{14}C$ curve inferred from German pine dendrochronology (*3, 22*), but this could not be confirmed by ice core data.

Our results falsify the concept of relatively stabilized Holocene CO_2 concentrations of 270 to 280 ppmv until the industrial revolution. SI-based CO_2 reconstructions may even suggest that, during the early Holocene, atmospheric CO_2 concentrations that were >300 ppmv could have been the rule rather than the exception (*23*).

References and Notes

1. D. Raynaud *et al.*, *Science* **259**, 926 (1993); H. Fischer, M. Wahlen, J. Smith, D. Mastroianni, B. Deck, *ibid.* **283**, 1712 (1999).
2. B. Stauffer *et al.*, *Nature* **392**, 59 (1998).
3. S. Björck *et al.*, *Science* **274**, 1155 (1996); S. Björck, M. Rundgren, Ó. Ingólfsson, S. Funder, *J. Quat. Sci.* **12**, 455 (1997).
4. R. B. Alley *et al.*, *Geology* **25**, 483 (1997).
5. Temporal resolution in Antarctic ice is sufficient, only for the past 600 years, to suggest a relation between a substantial CO_2 decline and the climate deterioration of the Little Ice Age [A. Indermühle *et al.*, *Nature* **398**, 122 (1999)].
6. M. J. M. Anklin, J. Barnola, B. Schwander, B. Stauffer, D. Raynaud, *Tellus Ser. B* **47**, 461 (1995); H. J. Smith, M. Wahlen, D. Mastroianni, K. C. Taylor, *Geophys. Res. Lett.* **24**, 1 (1997).
7. F. I. Woodward, *Nature* **327**, 617 (1987); ______ and F. A. Bazzaz, *J. Exp. Bot.* **39**, 1771 (1988); J. Peñuelas and R. Matamala, *ibid.* **41**, 1119 (1990); E. Paoletti and R. Gellini, *Acta Oecol.* **14**, 173 (1993); X. Q. He, Y. H. Lin, Y. X. Hu, *Chin. Sci. Bull.* **43**, 928 (1998).
8. J. Van Der Burgh, H. Visscher, D. L. Dilcher, W. M. Kürschner, *Science* **260**, 1788 (1993); W. M. Kürschner, J. Van Der Burgh, H. Visscher, D. L. Dilcher, *Mar. Micropaleontol.* **27**, 299 (1996).
9. F. Wagner *et al.*, *Proc. Natl. Acad. Sci. U.S.A.* **93**, 11707 (1996).
10. Stomatal index (SI) = [stomatal density/(stomatal density + epidermal cell density)] × 100.
11. I. Poole and W. M. Kürschner, in *Fossil Plants and Spores: Modern Techniques*, T. P. Jones and N. P. Rowe, Eds. (Geological Society, London, 1999), chap. 48.
12. I. Poole, J. D. B. Weyers, T. Lawson, J. A. Raven, *Plant Cell Environ.* **19**, 705 (1996).
13. Computer-aided determination of stomatal parameters on leaf cuticles was performed on a Leica Quantimet 500C/500+ Image Analysis System. Measured parameters include stomatal density and epidermal cell density (including stomatal guard cells). Counting areas were restricted to stomata-bearing alveoles. Calculated SI (*10*) are mean values for up to five leaves per horizon. Seven digitized images (field area, 0.035 mm^2) per leaf were analyzed (standard deviations are constant after seven counts).
14. F. Wagner *et al.*, in preparation. Field studies and growth experiments demonstrate that shade adaptation, expressed in leaf morphotype differentiation is diminished in the light-demanding pioneer species *B. pendula* and *B. pubescens*. The effects of a reduction of stomatal density as a result of epidermal cell expansion under shade conditions are compensated by applying the SI. Growth experiments also reveal that different nitrogen supply rates do not affect the stomatal frequency in tree birches, whereas increasing growth temperature under experimental conditions enhances stomatal initiation. Under natural conditions, changes in the phenological cycle of birches act as a filter for the potential effects of temperature changes on stomatal frequency.
15. C. D. Keeling, T. P. Whorf, M. Wahlen, J. Van Der Plicht, *Nature* **375**, 666 (1995); Cooperative Atmospheric Data Integration Project, *GLOBALVIEW-CO_2* (CD-ROM), (NOAA/CMDL, Boulder, CO, 1998) (available through anonymous ftp at ftp.cmdl.noaa.gov, path: ccg/co2/GLOBALVIEW).
16. W. M. Kürschner, F. Wagner, E. H. Visscher, H. Visscher, *Geol. Rundsch.* **86**, 512 (1997); W. M. Kürschner, F. Wagner, I. Stulen, P. J. C. Kuiper, *Ann. Bot.* **81**, 657 (1998).
17. D. J. Beerling, *Spec. Pap. Palaeontol.* **49**, 181 (1993); ______ and W. G. Chaloner, *Rev. Palaeobot. Palynol.* **81**, 11 (1994); P. K. Van De Water, S. W. Leavitt, J. L. Betancourt, *Science* **264**, 239 (1994); D. J. Beerling, H. H. Birks, F. I. Woodward, *J. Quat. Sci.* **10**, 379 (1995).
18. B. van Geel, S. J. P. Bohncke, H. Dee, *Rev. Palaeobot. Palynol.* **31**, 367 (1981).
19. T. Staffelbach, B. Stauffer, A. Sigg, *Tellus Ser. B* **43**, 91 (1991).
20. P. M. Grootes, M. Stuiver, J. W. C. White, S. J. Johnsen, J. Jouzel, *Nature* **366**, 552 (1993); M. Stuiver, P. M. Grootes, T. F. Braziunas, *Quat. Res.* **44**, 341 (1995).
21. A distinctive cooling pulse is not reflected in the Late Preboreal part of the pollen record of the Borchert section, suggesting that mild regional climatic conditions (*18*) prevented a detectable interruption in the forest development. Controversially, some authors (*3*) correlate the Preboreal Oscillation with the earlier Rammelbeek phase. There is strong evidence, however, that the characteristic expansion of grasses during this interval (Fig. 1A) was related to relatively warm dry summers rather than to cooling (*18*).
22. B. Kromer and B. Becker, *Radiocarbon* **35**, 125 (1993).
23. F. Wagner *et al.*, in preparation. Elevated early Holocene CO_2 concentrations have been replicated on the basis of *Betula* leaves from Holocene lake deposits in Denmark.
24. A. Neftel, E. Moor, H. Oeschger, B. Stauffer, *Nature* **315**, 45 (1985); H. Friedli, H. Lötscher, H. Oeschger, H. Siegenthaler, B. Stauffer, *ibid.* **324**, 237 (1986).

25. We thank B. Aaby, R. Below, and P. J. C. Kuiper for stimulating discussions and for constructive comments on the topic. Supported by the Deutsche Forschungsgemeinschaft (DFG) and the Council for Earth and Life Sciences (ALW) of the Netherlands Organization for Scientific Research (NWO). This is contribution 990501 from the Netherlands Research School of Sedimentary Geology and contribution 510 from the University of Florida Contributions to Paleobiology.

5 March 1999; accepted 17 May 1999

Contribution of Disturbance to Increasing Seasonal Amplitude of Atmospheric CO_2

S. A. Zimov,[1] S. P. Davidov,[1] G. M. Zimova,[1] A. I. Davidova,[1] F. S. Chapin III,[2*] M. C. Chapin,[2] J. F. Reynolds[3]

Recent increases in the seasonal amplitude of atmospheric carbon dioxide (CO_2) at high latitudes suggest a widespread biospheric response to high-latitude warming. The seasonal amplitude of net ecosystem carbon exchange by northern Siberian ecosystems is shown to be greater in disturbed than undisturbed sites, due to increased summer influx and increased winter efflux. Increased disturbance could therefore contribute significantly to the amplified seasonal cycle of atmospheric carbon dioxide at high latitudes. Warm temperatures reduced summer carbon influx, suggesting that high-latitude warming, if it occurred, would be unlikely to increase seasonal amplitude of carbon exchange.

Explaining recent changes in the global environment is a scientific challenge with important political and economic implications. Although increases in concentrations of greenhouse gases such as CO_2 and CH_4 have clear anthropogenic origins (*1*), the causes of the observed increased seasonal amplitude of atmospheric CO_2 are less clear. The increased amplitude is most pronounced at arctic and subarctic CO_2 monitoring stations (*2*) and largely reflects terrestrial carbon exchange at high latitudes (*3*). Two hypotheses have been advanced to explain this pattern: (i) The recent increase in March-April temperatures in high-latitude continental regions of North America and Siberia (*4*) could advance snowmelt and increase the length of the growing season (*2*), causing an increase in productivity and net ecosystem carbon gain (*5*); or (ii) temperature-driven increases in summer carbon gain balanced by increased winter respiration could enhance the seasonal amplitude of atmo-

[1]North-East Scientific Station, Pacific Institute for Geography, Far-East Branch, Russian Academy of Sciences, Republic of Sakha, Yakutia, 678830 Cherskii, Russia. [2]Institute of Arctic Biology, University of Alaska, Fairbanks, AK 99775–7000, USA. [3]Department of Botany, Duke University, Durham, NC 27708–0340, USA.

*To whom correspondence should be addressed. E-mail: fschapin@lter.uaf.edu